remote sensing

MDPI

Article

The Role of Subsurface Changes and Environmental Factors in Shaping Urban Heat Islands in Southern Xinjiang

Cong Wen [1,2,3,4,5], Hajigul Sayit [2,3,6], Ali Mamtimin [1,2,3,4,5,*], Yu Wang [1,2,3,4,5], Jian Peng [5,7], Ailiyaer Aihaiti [1,2,3,4,5], Meiqi Song [1,2,3,4,5], Jiacheng Gao [1,2,3,4,5], Junjian Liu [1,2,3,4,5], Yisilamu Wulayin [1,2,3,4,5], Fan Yang [1,2,3,4,5], Wen Huo [1,2,3,4,5] and Chenglong Zhou [1,2,3,4,5]

1 Institute of Desert Meteorology, China Meteorological Administration, Urumqi 830002, China; wencong@idm.cn (C.W.); wangyu@idm.cn (Y.W.); ailiyaer@idm.cn (A.A.); songmq@idm.cn (M.S.); gaojiach@idm.cn (J.G.); liujj@idm.cn (J.L.); yisilamu@idm.cn (Y.W.); yangfan@idm.cn (F.Y.); huowenpet@idm.cn (W.H.); zhoucl@idm.cn (C.Z.)
2 Xinjiang Key Laboratory of Desert Meteorology and Sandstorm, Urumqi 830002, China; hajigul@idm.cn
3 National Observation and Research Station of Desert Meteorology, Taklimakan Desert of Xinjiang, Urumqi 830002, China
4 Taklimakan Desert Meteorology Field Experiment Station of CMA, Urumqi 830002, China
5 Dabancheng National Special Test Field for Comprehensive Meteorological Observation, Urumqi 830002, China; pengjian@idm.cn
6 Xinjiang Meteorological Society, Urumqi 830002, China
7 Xinjiang Meteorological Technology Equipment Center, Urumqi 830001, China
* Correspondence: ali@idm.cn

Abstract: The urban heat island (UHI) effect is one of the most prominent surface climate changes driven by human activities. This study examines the UHI characteristics and influencing factors in the Southern Xinjiang urban agglomeration using MODIS satellite data combined with observational datasets. Our results reveal a significant increase in impervious surfaces in the region between 1995 and 2015, with the most rapid expansion occurring from 2010 to 2015. This urban expansion is the primary driver of changes in UHI intensity. The analysis from 2000 to 2015 shows substantial spatial variation in UHI effects across cities. Hotan recorded the highest annual average daytime UHI intensity of 3.7 °C, while Aksu exhibited the lowest at approximately 1.6 °C. Daytime UHI intensity generally increased during the study period, with the highest intensities observed in the summer. However, nighttime UHI trends varied across cities, with most showing an increase in intensity. Temperature, precipitation, and aerosol optical depth (AOD) were identified as the main factors influencing annual average daytime UHI intensity, while PM10 concentration showed a weak and inconsistent correlation with UHI intensity, varying by city and season.

Keywords: urban heat island; MODIS; AOD

check for updates

Citation: Wen, C.; Sayit, H.; Mamtimin, A.; Wang, Y.; Peng, J.; Aihaiti, A.; Song, M.; Gao, J.; Liu, J.; Wulayin, Y.; et al. The Role of Subsurface Changes and Environmental Factors in Shaping Urban Heat Islands in Southern Xinjiang. *Remote Sens.* **2024**, *16*, 4089. https://doi.org/10.3390/rs16214089

Academic Editor: Stefania Bonafoni

Received: 1 October 2024
Revised: 21 October 2024
Accepted: 30 October 2024
Published: 1 November 2024

Copyright: © 2024 by the authors. Licensee MDPI, Basel, Switzerland. This article is an open access article distributed under the terms and conditions of the Creative Commons Attribution (CC BY) license (https://creativecommons.org/licenses/by/4.0/).

1. Introduction

Urban areas serve as political, economic, and cultural hubs, acting as major gathering points for human populations. However, urbanization introduces significant changes to the local climate, primarily due to alterations in land use and increased pollutant emissions. These changes lead to a phenomenon known as the Urban Heat Island (UHI), whereby the temperature in urban areas exceeds that of the surrounding rural regions [1]. The UHI effect is one of the most profound surface climate change effects resulting from human activities. Since Harold's seminal observation in 1833 that the temperature in central London was higher than that in its suburbs [2], the UHI effect has garnered significant attention. This is not only due to its potential to degrade the quality of life but also because of its capacity to exacerbate energy consumption, air pollution, and the frequency of heatwave events in urban environments [3–6].

In recent years, research on the urban heat island effect follows a significant growth trend [7], and some of the heat island effect studies mainly utilize the observation data from meteorological stations [8–11]; however, due to the limited number of stations and their uneven spatial distribution, there are some limitations on the study of heat island effect [12]. Therefore, more scholars choose satellite data for research [13–15], and satellite thermal infrared remote sensing is the main method used to obtain the surface temperature (86.5%) [12], which mainly focuses on the study of spatial and temporal characteristics of the urban heat island [16–19]. Using remote sensing technology and ground observation data, researchers have derived detailed spatial distribution maps and temporal trends of heat island effects in the region. For example, MODIS and Landsat satellite data have been widely used to monitor urban surface temperatures, revealing the difference in temperature between urban centers and the surrounding rural areas, and how this difference varies with the seasons and the degree of urbanization [20–24]. In addition to this, the use of models for the study of urban heat islands is also a common approach [25,26], and some studies have investigated the impact of land use on the heat island effect by establishing a surface heat island model [27] and a spatial regression model [28]. Moreover, urban morphology variables were utilized to predict the urban heat island effect in Europe [29].

The influencing factors of the urban heat island effect are more complicated [30–32]; therefore, the influencing factors of the change in urban heat island effect intensity have been a hot research issue [32,33]. Meteorological variables, including relative humidity, cumulative precipitation, and aerosol optical thickness have the most significant influence on the intensity of the heat island effect [34]. In-depth study of the influence mechanism of these factors on the heat island effect and the development of corresponding regulatory measures are of great significance for mitigating the heat island effect and improving the quality of the urban environment. Although more scholars have focused on the study of the urban heat island effect at home and abroad, there is still a large gap in the study of the urban climate effect in the Xinjiang region [35], and there are only a few studies on the urban heat island in Urumqi [36–39]. There have been studies on the characteristics of urban heat island in semi-arid regions [40] and spatial and temporal analyses of the urban heat island near deserts [41–43]. As an important economic and cultural center in western China, the southern urban agglomeration of Xinjiang has experienced rapid urbanization in recent years. With urban expansion and population growth, the urban heat island effect has become one of the notable environmental problems facing the region. The Southern Xinjiang urban agglomeration with Kashgar as the regional center has faced more serious air pollution problems in recent years [44,45]; however, there are still few studies on the Southern Xinjiang urban agglomeration exploring its urban climate effect and other related issues, and there is an urgent need for studies on the heat island of the Southern Xinjiang urban agglomeration to provide the scientific basis for decision-making relating to urban construction. Therefore, it is important to study the heat island effect in the Southern Xinjiang urban agglomeration, especially its spatial and temporal characteristics and influencing factors, in order to formulate effective urban planning and environmental protection policies.

This study aims to investigate the spatial and temporal characteristics of the UHI effect in the Southern Xinjiang urban agglomeration. Using MODIS surface temperature synthesis products, we analyze the influencing factors of UHI intensity, including precipitation, air temperature, AOD, and pollutant concentrations. The goal is to contribute to the formulation of effective urban planning and environmental protection policies for the region.

2. Materials and Methods

2.1. Study Area

The urban agglomeration of Southern Xinjiang, centered on Kashgar, is distributed around the Tarim Basin (Figure 1), including Kashgar, Hotan, Atushi, Aksu, and Korla. These cities are the region of rapid population concentration and economic development

in the Southern Xinjiang region. For example, Kashgar is located in the southwestern part of Xinjiang Uygur Autonomous Region and the western edge of the Tarim Basin, with a warm-temperate continental arid climate and four distinct seasons, covering a total area of 1056.8 km^2. Hotan is located in the southwestern part of Xinjiang Uygur Autonomous Region between the Karakorum Mountains and the Taklamakan Desert, with an arid desert climate and a total area of 585.11 km^2. Korla is located in the central part of Xinjiang, at the southern foot of the Tianshan Mountain and the northeastern edge of the Tarim Basin, relying on the branch of the Tianshan Mountain in the north, and facing the Taklamakan Desert, the second largest desert in the world, in the south. It is a key point of the middle road of the ancient Silk Road and one of the birthplaces of Western culture, serving as an important transportation hub and material distribution center of the North and South Xinjiang.

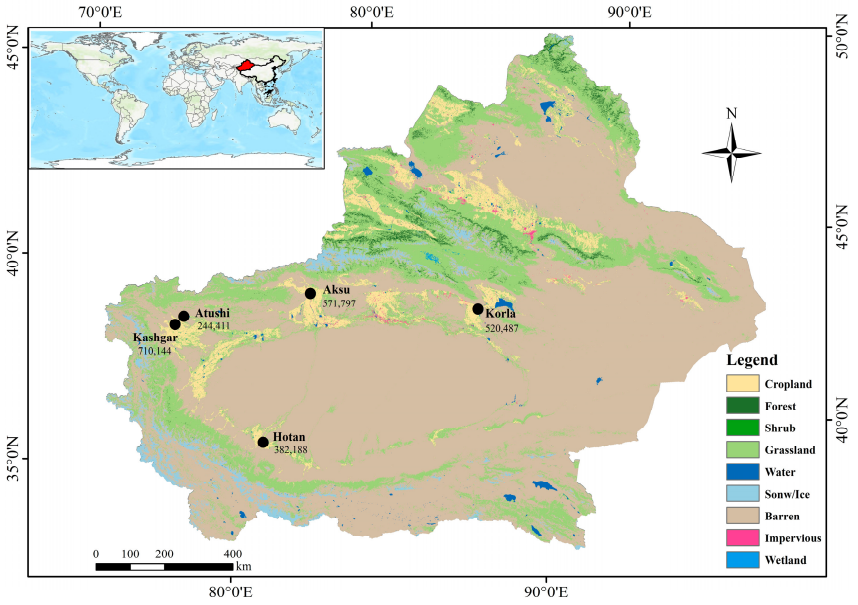


Figure 1. Map of urban agglomeration distribution in South Xinjiang (the number under the city name represents the population in that city in 2015).

According to the approach for selecting urban and surrounding rural image points [34], the selection of points in this study follows the principle that the difference in latitude between urban image points and rural image points is no more than 0.1°, the difference in altitude is no more than 100 m, and the type of land use is fully considered [46]. Detailed point selection is shown in Table 1.

Table 1. Station information.

	Station Type	Station	Longitudes (°)	Latitude (°)	Altitude (m)
Hotan	City Center	51828	79.93	37.13	1375
	Rural Region	Y6229	79.89	37.1	1304
Kashgar	City Center	Y9199	75.97	39.45	1289.4
	Rural Region	Y9188	75.97	39.39	1277
Atushi	City Center	Y8996	76.17	39.72	1298.7
	Rural Region	51704	76.22	39.73	1267.6
Aksu	City Center	Y8677	80.23	41.16	1103.8
	Rural Region	Y5930	80.2	41.03	1081
Korla	City Center	Y8332	86.16	41.71	892
	Rural Region	Y8334	86.08	41.67	914

2.2. Data Sources

Due to the most rapid increase in urban impervious cover area in Southern Xinjiang from 2010 to 2015 and the limitations of the data time scale, this study examines the seasonal variations in the urban heat island (UHI) effect using surface temperature data from 2000 to 2015. The data were obtained from the monthly synthesized 1 km surface temperature products, MODLT1M and MYDLT1M, provided by the Geospatial Data Cloud Platform of the Chinese Academy of Sciences Computer Network Information Center (http://www.gscloud.cn, accessed on 22 April 2024). These products, MODLT1T and MYDLT1D, were synthesized by calculating the monthly average surface temperature values with a spatial resolution of 1 km. For the purposes of this study, the meteorological seasons were defined as follows: March to May for spring, June to August for summer, September to November for autumn, and December to February for winter. In this study, the pixel point represents where the weather station is located is, based on the latitude and longitude data of the weather station, and the temperature value of the pixel point is used to represent the temperature at the weather station.

The PM10 data were sourced from the National Tibetan Plateau Science Data Center (http://data.tpdc.ac.cn, accessed on 10 June 2024). This dataset employs artificial intelligence techniques to fill in missing spatial values from MODIS MAIAC Aerosol Optical Depth (AOD) products. It combines ground-based observations, atmospheric reanalysis, and emission inventories with big data production to generate seamless, high-resolution ground-level PM10 data for the entire country, with a spatial resolution of 1 km, covering the period from 2000 to the present [47,48].

Additionally, precipitation and temperature data were acquired from the National Tibetan Plateau Science Data Center (http://data.tpdc.ac.cn, accessed on 8 July 2024), with a spatial resolution of 0.0083333° [49]. Data on impervious surfaces were retrieved from the StarCloud Data Platform (https://data-starcloud.pcl.ac.cn/zh/resource/13, accessed on 23 July 2024) [50]. Population data for the same period were obtained from a query based on the China Urban Statistical Yearbook. Data on nighttime lighting were obtained from NOAA (https://www.ngdc.noaa.gov/eog/viirs/download_ut_mos.html, accessed on 2 September 2024). Finally, AOD data were obtained from the MODIS Level 2 MYD08 product [51].

2.3. Research Methodology

2.3.1. Urban Heat Island Intensity (UHII)

According to the definition of the urban heat island, urban heat island intensity (UHII) is the difference between the surface temperature of the city and the surface temperature of the surrounding rural areas:

$$UHII = T_U - T_R \quad (1)$$

Here, T_U represents the surface temperature of the city, and T_R represents the surface temperature of the surrounding rural areas.

2.3.2. Correlation Coefficient

In order to study the influencing factors of urban heat island intensity in the urban agglomeration of South Xinjiang, this paper uses the data of air temperature, precipitation, PM10, and AOD, and the Pearson correlation coefficient method is used to calculate the correlation between each factor and the urban heat island intensity, which is calculated by the following formulas:

$$r = \frac{\sum_1^n (x_i - \overline{x})(y_i - \overline{y})}{\sqrt{\sum_{i=1}^n (x_i - \overline{x})^2}\sqrt{\sum_{i=1}^n (y_i - \overline{y})^2}} \quad (2)$$

Here, x_i and y_i represent the values of the two variables, $\overline{x}$ and $\overline{y}$ represent the means of the two variables, respectively, and n represents the sample size.

3. Results

3.1. Development Process of Urban Agglomerations in Southern Xinjiang

As shown in Figure 2, the impervious surfaces in the Southern Xinjiang urban agglomeration experienced a notable increase between 1995 and 2015. Figure 3 illustrates the change in the area and spatial distribution of impervious surfaces by city in 1995 and 2015. Over this 20-year period, the non-cultivated area expanded significantly, growing from 1.84 km^2 to 22.95 km^2. Among the regions, Aksu exhibited the largest increase in impervious surface, with an expansion of 6.78 km^2, followed by Kashgar, which saw an increase of 4.51 km^2. The most substantial growth in impervious surfaces occurred during the 2010–2015 period, coinciding with rapid urbanization. Therefore, it is of representative significance for urban planning in Southern Xinjiang to study the influence factors and change characteristics of the urban heat island effect in the period 2000–2015. This expansion of impervious surfaces is expected to alter the thermal characteristics of the urban environment, contributing to an increase in the intensity of the urban heat island (UHI) effect. The growing impervious surface area reduces the natural capacity of the landscape to absorb and dissipate heat, which amplifies the UHI effect and contributes to changes in the city's thermal dynamics.

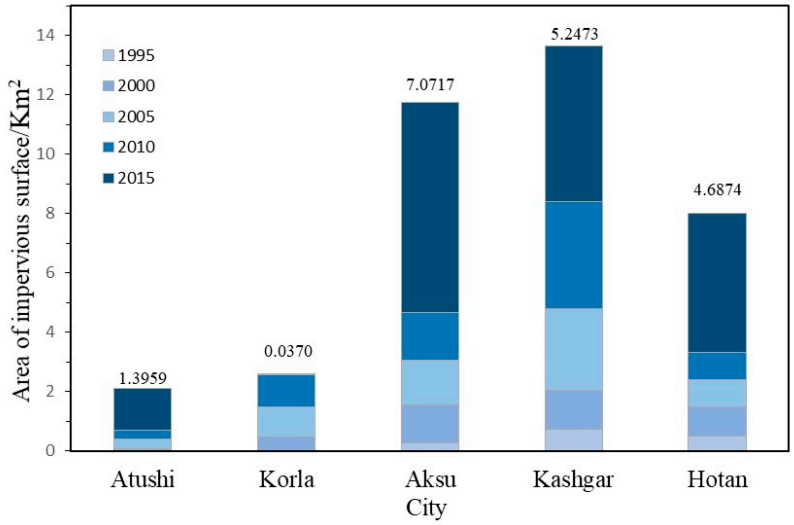


Figure 2. Trends in impervious surface changes in the South Xinjiang urban agglomeration, 1995–2015.

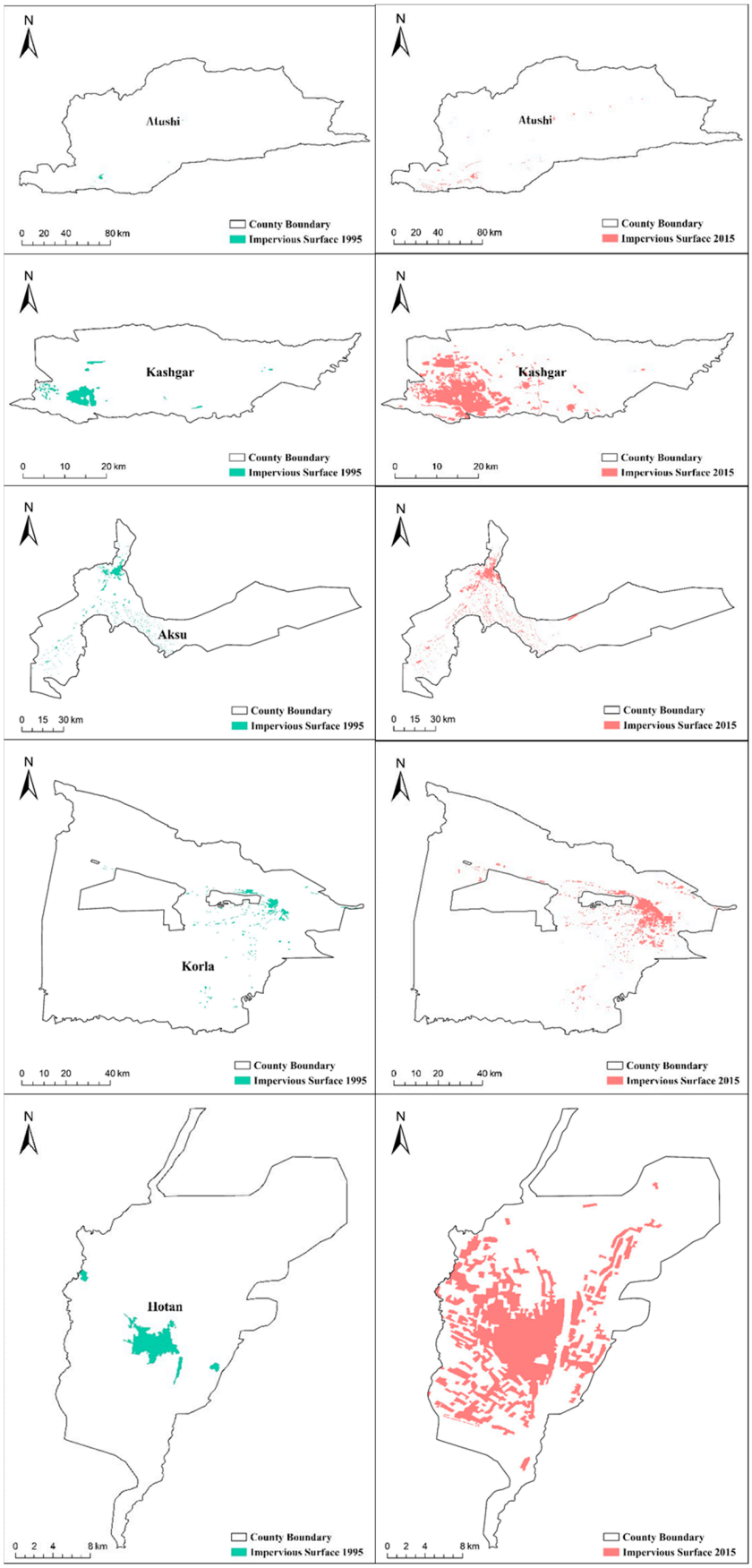


Figure 3. Spatial changes in impervious surface in the Southern Xinjiang urban agglomeration, 1995–2015.

3.2. Characterization of Changes in the Urban Land Surface Temperature

In order to understand the spatial distribution of the urban thermal environment more easily, Figures 4 and 5 show the spatial distribution characteristics of surface temperature in the southern border urban agglomeration in 2000, 2005, 2010, and 2015. Combined with the analysis of the spatial change in the impervious layer in Figure 3, we can find that with the development process of urbanization, the high value area of the daytime surface temperature in each city is transformed from a more dispersed area to a gradually concentrated area towards the city center, and it is consistent with the area where the impervious layer increases. The nighttime urban surface temperature is lower compared with the daytime but shows a very obvious distribution of high value areas in the urban center.

This indicates that the heat island effect during daytime and nighttime in the South Xinjiang urban agglomeration gradually increased during the period 2000–2015, and the spatial high value areas gradually converged to the urban centers.

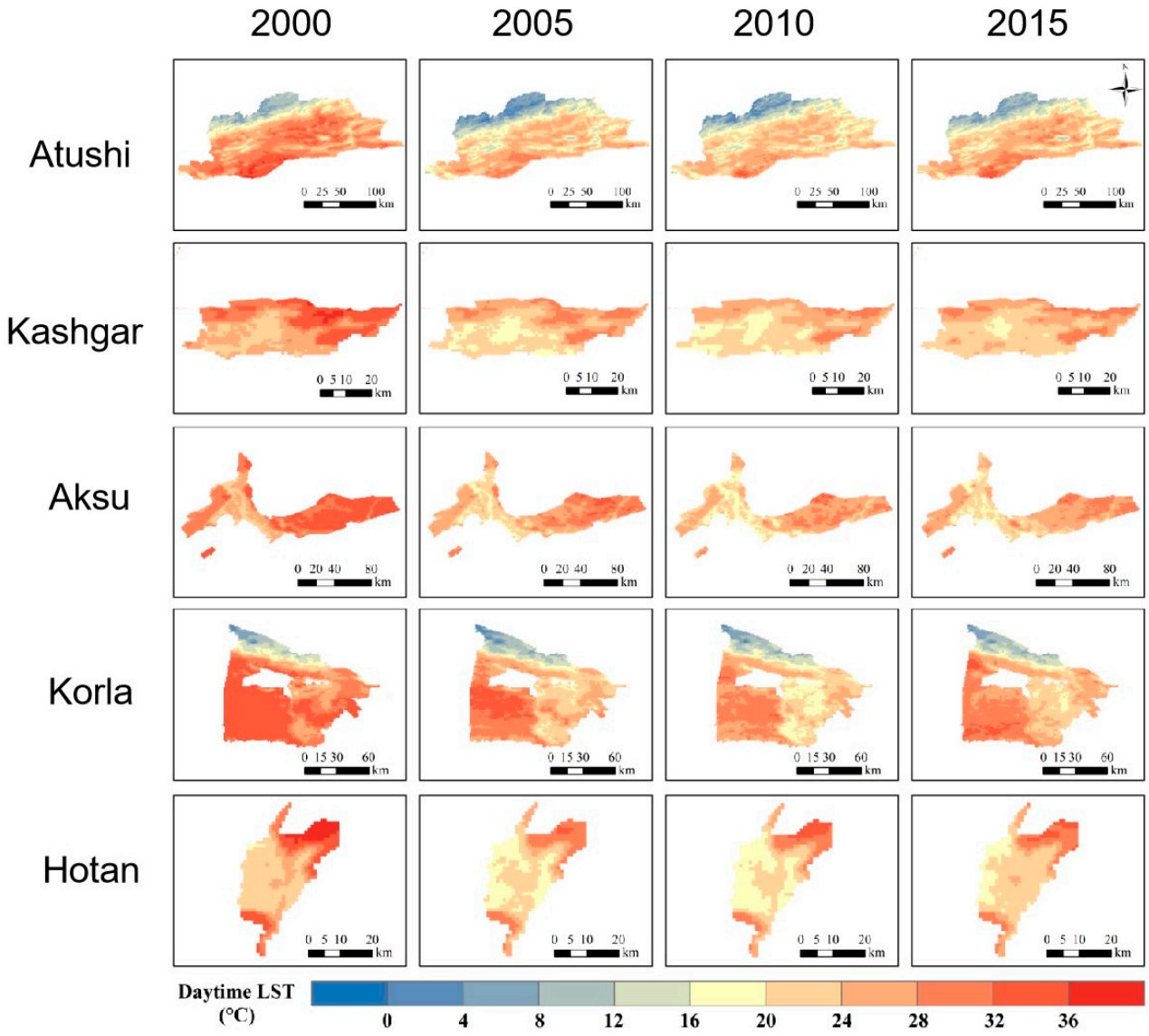


Figure 4. Characteristics of daytime land surface temperature changes in urban agglomerations in South Xinjiang.

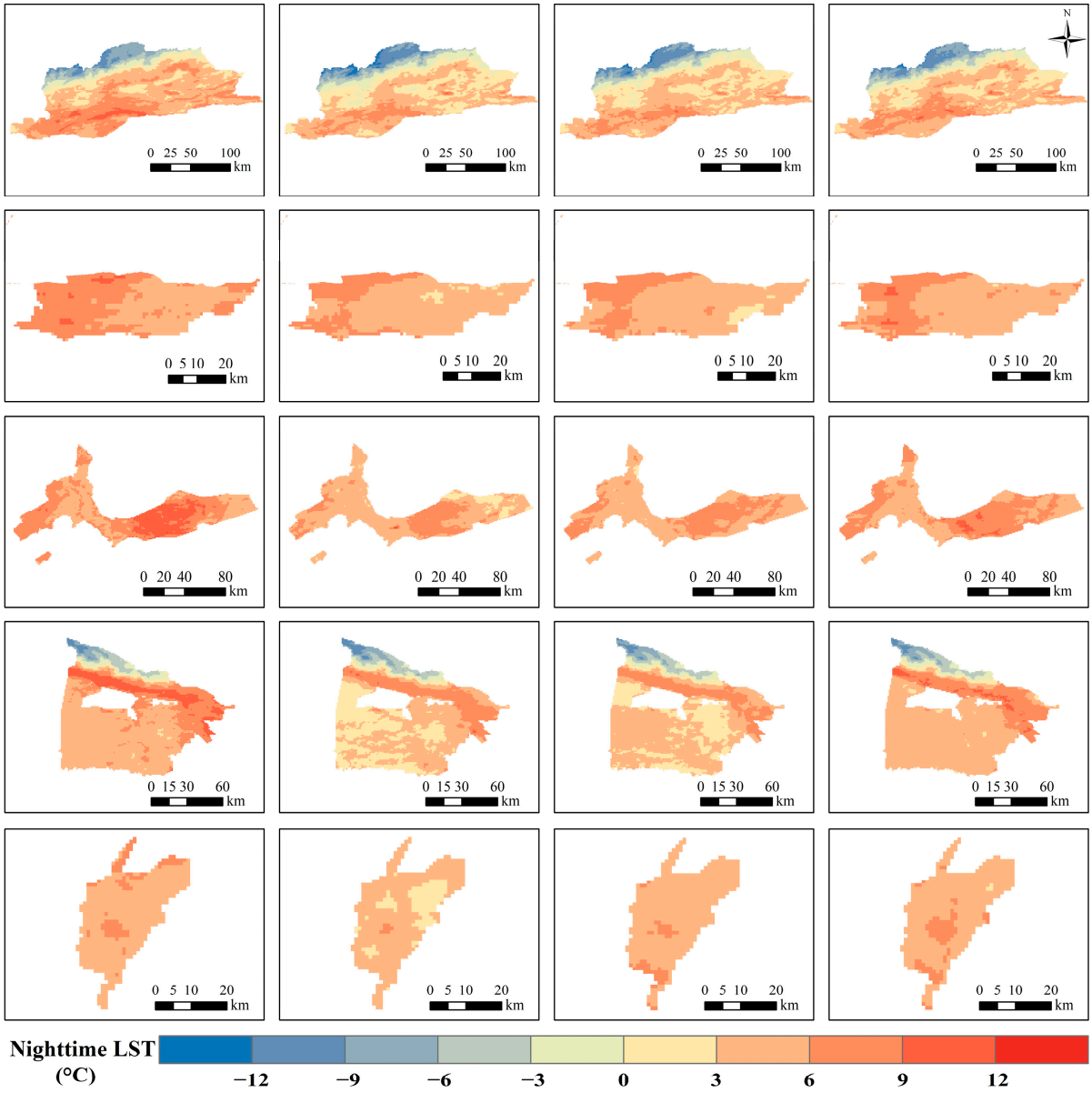


Figure 5. Characteristics of nighttime land surface temperature changes in urban agglomerations in South Xinjiang.

3.3. Characteristics of Urban Heat Island Variation in South Xinjiang Urban Agglomeration

Figures 6 and 7 illustrate the spatial distribution of urban heat island (UHI) intensity during both daytime and nighttime across the Southern Xinjiang urban agglomeration from 2000 to 2015. The analysis reveals significant spatial variability in UHI intensity among different cities. The heat island effect is present in all cities during both daytime and nighttime, with an average daytime UHI intensity of 2.15 °C and a nighttime average of 2.09 °C.

During the daytime, Hotan exhibited the highest UHI intensity at 3.4 °C, while Aksu recorded the lowest at 1.6 °C. In Kashgar, the UHI intensity was 2.15 °C during the day and 2.09 °C at night. Nighttime UHI was most pronounced in Kashgar, where the intensity reached 3.4 °C, compared to Hotan, which had the lowest nighttime intensity of 0.67 °C.

Seasonal variations in UHI intensity were also evident (Table 2). Kashgar experienced the highest daytime and nighttime UHI intensities in both summer and autumn. During winter, Kashgar maintained the highest nighttime UHI intensity, and the following interesting phenomenon was observed: the occurrence of a "cold island" effect during the daytime

in both Kashgar and Hotan. This anomaly is likely due to the proximity of these cities to the desert, where the low vegetation cover in the surrounding rural areas increases the efficiency of sensible heat exchange, leading to the cold island effect.

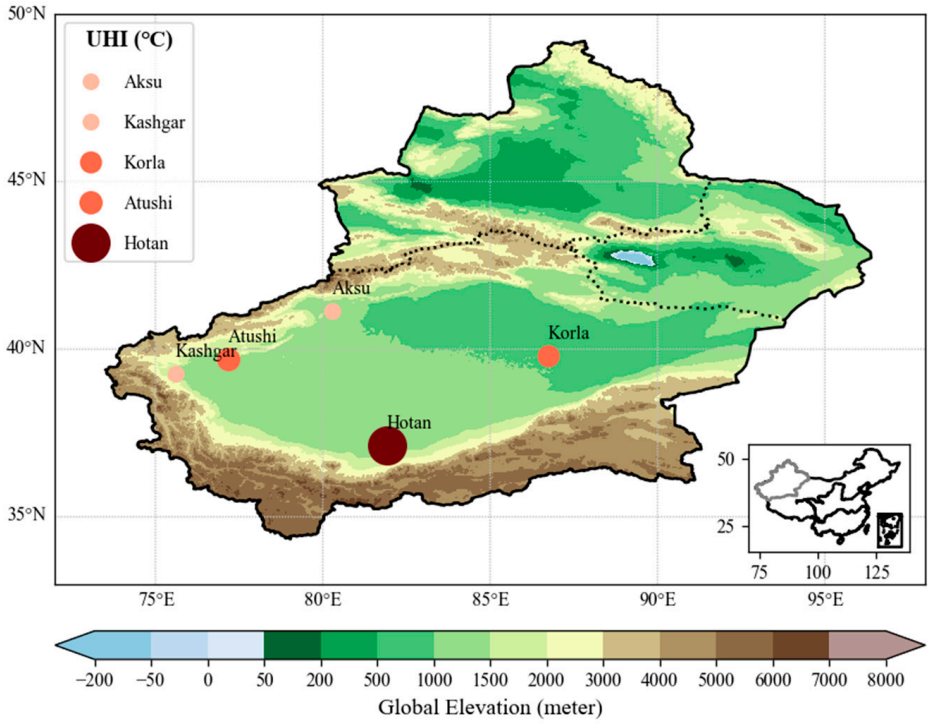


Figure 6. Spatial distribution of urban heat island intensity in urban agglomerations in South Xinjiang during daytime.

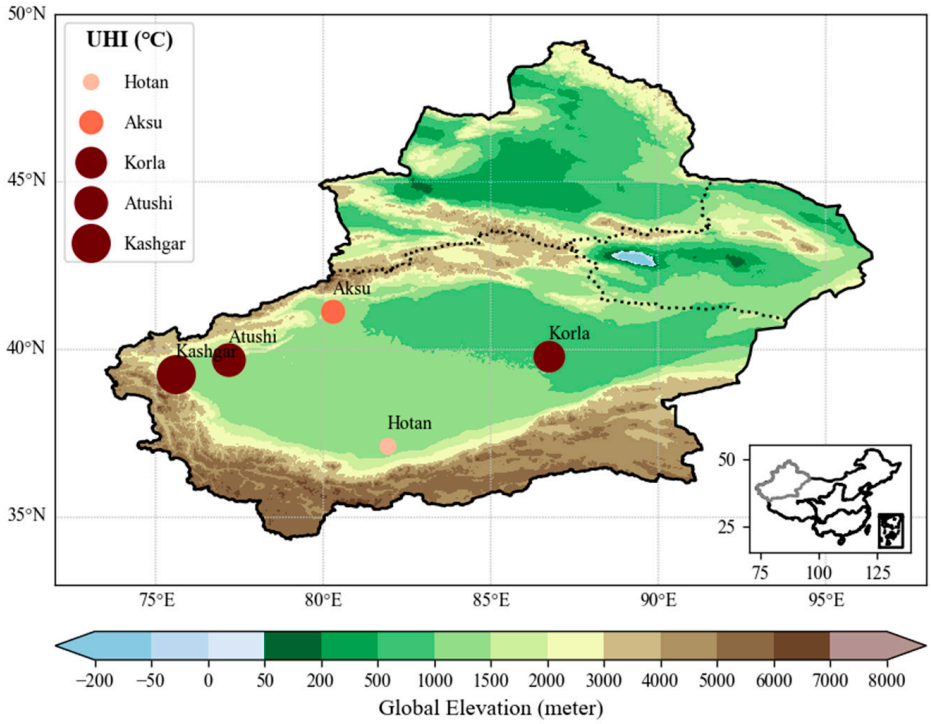


Figure 7. Spatial distribution of urban heat island intensity in urban agglomerations in South Xinjiang during nighttime.

Table 2. Seasonal variation in urban heat island intensity in the urban agglomeration of South Xinjiang (°C).

City	Time	UHII-Spring	UHII-Summer	UHII-Autumn	UHII-Winter
Hotan	Day	0.90	3.81	1.33	−0.07
	Night	0.39	1.20	0.82	0.34
Kashgar	Day	0.80	6.18	2.01	−1.12
	Night	2.46	3.40	3.56	3.52
Korla	Day	0.35	1.23	0.41	1.30
	Night	2.40	3.02	2.43	1.69
Aksu	Day	0.57	3.51	1.07	0.84
	Night	1.34	2.08	1.76	0.94
Atushi	Day	1.94	4.41	1.85	0.24
	Night	2.46	2.69	2.84	2.44

In summary, the highest daytime UHI intensities in all cities were recorded during the summer, while nighttime UHI intensities, although present across all cities, exhibited relatively smaller seasonal fluctuations.

The heat island intensity in the Southern Xinjiang urban agglomeration exhibited notable inter-annual variability, influenced by changes in the impervious surface area, population growth, and other factors (Figure 8). From 2000 to 2015, the daytime UHI intensity in all cities showed an overall increasing trend, with Kashgar experiencing the most pronounced increase. Hotan consistently recorded the highest daytime UHI intensity during this period, with a sharp increase observed after 2010.

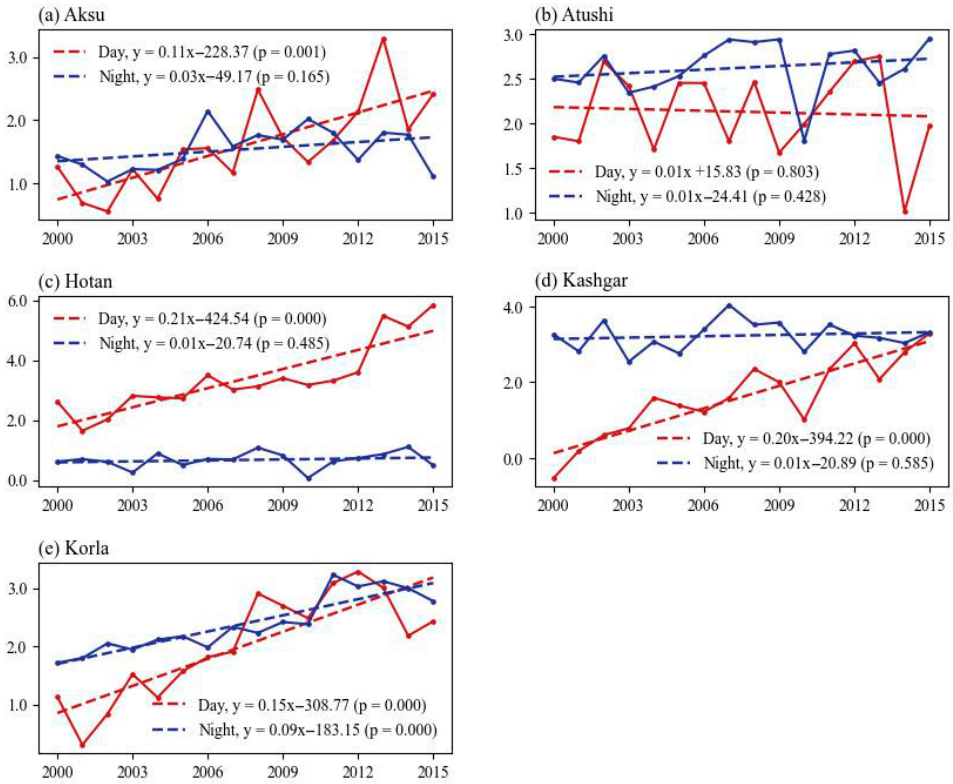


Figure 8. Annual variation in urban heat island intensity in the South Xinjiang urban agglomeration, 2000–2015 ((**a**). Aksu, (**b**). Atushi, (**c**). Hotan, (**d**). Kashgar, (**e**). Korla).

The trend in daytime UHI intensity across the agglomeration can be divided into three distinct phases as follows: an initial increase from 2000 to 2005, followed by a slight decline between 2005 and 2010, and a subsequent rapid rise from 2010 to 2015.

In contrast, the trends in nighttime UHI intensity varied more across cities. Meanwhile, most cities saw an increase in nighttime UHI intensity from 2000 to 2015, Among them, during the daytime, Aksu, Hotan, Kashgar, and Korla all showed significant growth trends ($p < 0.01$). Kashgar, in particular, consistently exhibited strong nighttime UHI intensities, ranging between 2.5 °C and 3.5 °C throughout the 15-year period. The main reason for this is that Kashgar has a higher and denser increase in the area of impervious cover and has the largest population. In contrast, the urbanization process in Atushi is slower, and the increasing trend of heat island intensity is not significant.

Figure 9 illustrates the seasonal changes in daytime and nighttime urban heat island intensity in the Southern Xinjiang urban agglomeration from 2000 to 2015, revealing distinct seasonal patterns across cities. These variations highlight the significant influence of seasonality on the UHI effect.

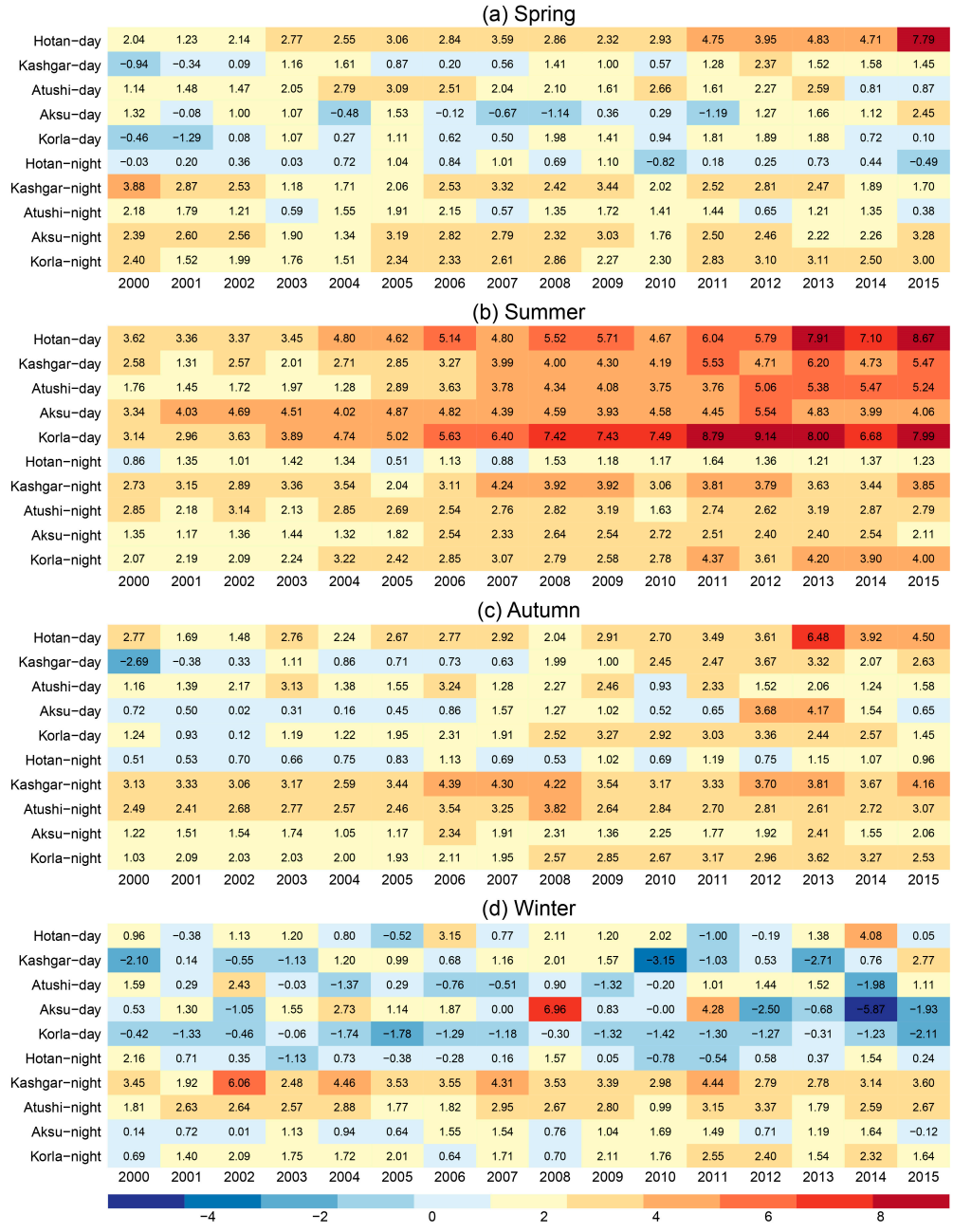


Figure 9. Seasonal variation in urban heat island intensity in the South Xinjiang urban agglomeration, 2000–2015 ((**a**). Spring, (**b**). Summer, (**c**). Autumn, (**d**). Winter).

In general, the daytime UHI intensity across the urban agglomeration exhibits an upward trend during spring, although a slight decline is observed in a few cities. Hotan consistently maintains a higher intensity during this season, with UHI values reaching a maximum of 7.8 °C, the largest increase during the period. The summer season also shows a clear upward trend in daytime UHI intensity, particularly in Hotan and Korla, where consistently high values are recorded.

During autumn, the increase in daytime UHI intensity is more pronounced, with Hotan and Korla again showing higher values, while Kashgar experiences the greatest increase in intensity. In winter, the trend becomes more complex, with daytime UHI intensity fluctuating or increasing, depending on the city. Overall, the daytime UHI intensity in the Southern Xinjiang urban agglomeration follows a consistent pattern of higher values in the spring and summer, while autumn and winter exhibit more variability and fluctuations.

At night, the UHI intensity also demonstrates seasonal variation. In spring, nighttime UHI intensity fluctuates across the region, with a general upward trend observed in most cities, particularly in Atushi and Kashgar. The summer season shows a more consistent upward trend in nighttime UHI intensity across the agglomeration. In autumn, the nighttime UHI intensity continues to rise, with Kashgar maintaining the highest values, ranging from 3 °C to 4.2 °C. Winter, however, presents more variation, with fluctuations in nighttime UHI intensity across cities. Hotan, in particular, shows a noticeable downward trend during winter, while Kashgar consistently records higher values, exceeding 3 °C.

In summary, the seasonal changes in nighttime UHI intensity are marked by smoother trends during autumn, while spring and winter show more pronounced fluctuations. Overall, the data suggest that both daytime and nighttime UHI intensities are influenced by seasonal factors, with spring and summer generally exhibiting higher values, and autumn and winter showing greater complexity and variability.

3.4. Relationship Between Urban Heat Islands and Their Influencing Factors

To explore the associations between various environmental variables and heat island intensity in the Southern Xinjiang urban agglomeration, a correlation analysis was conducted, examining the relationships between nighttime light, population, impervious surfaces, temperature, precipitation, PM10, aerosol optical depth (AOD), and heat island intensity (Table 3). The results indicate significant statistical associations, suggesting that the annual average daytime heat island intensity in the southern border cities is closely linked to variations in nighttime light, population, impervious surfaces, temperature, precipitation, and AOD.

Table 3. Correlation of heat island intensity and its influencing factors in the Southern Xinjiang urban agglomeration, 2000–2015.

(a)

Aksu	Average Annual Daytime	Spring Daytime	Summer Daytime	Autumn Daytime	Winter Daytime	Average Annual Nighttime	Spring Nighttime	Summer Nighttime	Autumn Nighttime	Winter Nighttime
Nighttime Light	0.736 **	0.398	0.866 ***	0.658 **	−0.571 *	0.209	−0.485	0.572 *	0.487	0.150
Population	0.713 **	0.093	0.851 ***	0.500 *	−0.237	0.413	−0.432	0.775 ***	0.464	0.443
Impervious Surfaces	0.786 ***	0.145	0.959 ***	0.563 *	−0.345	0.446	−0.396	0.830 ***	0.535 *	0.339
Temperature	0.340 ***	−0.537 ***	0.598 ***	0.420 **	0.253	0.379 ***	0.119	0.328 *	0.439 **	−0.300 *
Precipitation	0.316 ***	−0.155	0.133	0.246	0.174	0.243 ***	−0.054	−0.003	0.339 *	0.049
PM10	−0.007	0.205	−0.261	−0.053	0.206	−0.078	−0.156	−0.351 *	0.054	0.153
AOD	0.166	0.095	−0.521 **	−0.170	0.538 *	0.177	0.003	−0.352	−0.170	0.538 *

Table 3. *Cont.*

(b)										
Atushi	Average Annual Daytime	Spring Daytime	Summer Daytime	Autumn Daytime	Winter Daytime	Average Annual Nighttime	Spring Nighttime	Summer Nighttime	Autumn Nighttime	Winter Nighttime
Nighttime Light	0.060	−0.109	0.334	−0.162	0.093	0.154	0.077	0.126	0.158	0.113
Population	−0.053	−0.100	0.280	−0.114	−0.091	0.195	0.077	0.212	0.138	0.155
Impervious Surfaces	−0.057	−0.055	0.275	−0.073	−0.130	0.259	0.156	0.121	0.372	0.132
Temperature	0.729 ***	0.789 ***	−0.000	0.815 ***	−0.148	−0.145 *	0.327 *	0.275	−0.107	−0.287
Precipitation	0.465 ***	0.434 **	0.143	0.411 **	0.259	−0.014	−0.228	−0.271	−0.330 *	0.107
PM10	−0.084	−0.207	−0.107	0.175	−0.185	0.124	0.049	0.035	0.509 ***	0.238
AOD	−0.133	−0.231	−0.206	−0.364 *	0.061	0.266 **	0.313	−0.338	−0.364 *	0.061
(c)										
Hotan	Average Annual Daytime	Spring Daytime	Summer Daytime	Autumn Daytime	Winter Daytime	Average Annual Nighttime	Spring Nighttime	Summer Nighttime	Autumn Nighttime	Winter Nighttime
Nighttime Light	0.835 ***	0.864 ***	0.873 ***	0.663 **	0.120	0.086	−0.183	0.280	0.592 *	−0.154
Population	0.831 ***	0.756 ***	0.877 ***	0.714 **	0.180	0.238	0.049	0.177	0.623 **	−0.087
Impervious Surfaces	0.757 ***	0.703 **	0.840 ***	0.626 **	0.168	0.219	−0.030	0.333	0.568 **	−0.092
Temperature	0.646 ***	0.473 ***	0.175	0.297 *	0.356 *	0.318 ***	0.250	0.440 **	0.596 ***	−0.131
Precipitation	0.263 ***	0.296 *	−0.124	0.205	−0.170	0.108	0.046	−0.162	0.279	0.065
PM10	0.025	0.012	−0.093	−0.099	0.260	−0.079	−0.087	0.182	−0.225	−0.043
AOD	0.040	0.014	−0.354	0.070	0.084	0.459 ***	0.494 **	−0.280	0.070	0.084
(d)										
Kashgar	Average Annual Daytime	Spring Daytime	Summer Daytime	Autumn Daytime	Winter Daytime	Average Annual Nighttime	Spring Nighttime	Summer Nighttime	Autumn Nighttime	Winter Nighttime
Nighttime Light	0.847 ***	0.744 ***	0.840 ***	0.878 ***	0.030	0.028	−0.339	0.440	0.357	−0.145
Population	0.897 ***	0.842 ***	0.797 ***	0.846 ***	0.226	0.002	−0.402	0.459	0.450	−0.207
Impervious Surfaces	0.860 ***	0.689 **	0.908 ***	0.822 ***	0.163	0.304	−0.106	0.637 **	0.522 *	−0.085
Temperature	0.466 ***	−0.485 ***	0.387 **	0.377 **	−0.227	−0.159 *	0.326 *	0.171	−0.059	−0.375 *
Precipitation	0.252 ***	0.116	0.030	0.286 *	0.068	−0.001	−0.441 **	−0.136	−0.273	0.153
PM10	−0.025	0.043	0.071	−0.176	0.265	0.029	−0.332 *	−0.059	0.364 *	0.064
AOD	−0.067	0.327	−0.324	−0.307	−0.429	0.048	−0.235	−0.619 ***	−0.307	−0.429
(e)										
Korla	Average Annual Daytime	Spring Daytime	Summer Daytime	Autumn Daytime	Winter Daytime	Average Annual Nighttime	Spring Nighttime	Summer Nighttime	Autumn Nighttime	Winter Nighttime
Nighttime Light	0.859 ***	0.597 *	0.916 ***	0.700 **	−0.206	0.927 ***	0.783 ***	0.858 ***	0.852 ***	0.415
Population	0.725 **	0.535 *	0.767 ***	0.552 *	−0.263	0.812 ***	0.678 **	0.813 ***	0.728 **	0.338
Impervious Surfaces	0.841 ***	0.579 *	0.907 ***	0.712 **	−0.329	0.860 ***	0.774 ***	0.822 ***	0.809 ***	0.330
Temperature	0.785 ***	0.379 **	0.270	0.807 ***	0.062	0.064	0.190	0.140	0.485 ***	0.251
Precipitation	0.606 ***	0.295 *	−0.190	0.456 **	0.098	0.043	0.279	−0.128	0.125	−0.278
PM10	−0.109	−0.142	−0.178	0.048	−0.172	0.035	0.020	−0.045	−0.137	−0.101
AOD	0.122	0.278	−0.265	−0.124	0.236	0.528 ***	0.588 ***	−0.400 *	−0.124	0.236

(a) Aksu (b) Atushi (c) Hotan (d) Kashgar (e) Korla. *** represents significance $p < 0.001$, ** represents significance $p < 0.01$, * represents significance $p < 0.05$.

From a seasonal perspective, a strong positive association between spring daytime heat island intensity and temperature is evident across the region. However, during the summer, some cities exhibit a negative correlation between daytime heat island intensity and AOD. Notably, no strong associations were observed between any variables and daytime heat island intensity in the autumn and winter.

Temperature shows the strongest association with annual average nighttime heat island intensity in the Southern Xinjiang urban agglomeration. Additionally, precipitation is significantly positively associated with nighttime heat island intensity in Aksu. In spring, air temperature is positively correlated with nighttime heat island intensity in Atushi and Kashgar, while precipitation in Kashgar shows a negative association with spring nighttime UHI intensity. In the autumn, nighttime UHI intensity in Aksu, Hotan, and Korla is significantly positively correlated with air temperature. Anthropogenic factors such as nighttime light, population, impervious surfaces, etc., are strongly correlated with heat island intensity in the Southern Xingjiang urban agglomerations, and the results are significant

The correlation between PM10 concentration and UHI intensity is generally weak and varies across cities and seasons. For instance, in Atushi and Kashgar, PM10 shows a significant positive association with nighttime heat island intensity during the autumn.

4. Discussion

This study examined the spatiotemporal variations in urban heat island (UHI) intensity across the Southern Xinjiang urban agglomeration, identifying key influencing factors such as temperature, precipitation, PM10, and aerosol optical depth (AOD). The findings reveal significant UHI phenomena in all cities, with notable variations between regions and seasons. A unique feature of this region, however, is the occurrence of a "cold island" phenomenon in Kashgar and Hotan during winter daytime hours. This contrasts with typical UHI behavior observed in other urban centers.

The cold island phenomenon observed during winter daytime in Kashgar and Hotan results from a combination of factors, including reduced solar radiation, shading from urban morphology, differences in heat absorption between urban and rural areas, atmospheric stability, and the unique characteristics of the surrounding desert. The combined effects of these factors create a situation where rural areas, particularly the desert, absorb more heat during the day, leading to higher temperatures compared to cooler, shaded urban areas. This thermal contrast is further amplified by seasonal changes in atmospheric circulation and reduced anthropogenic heat emissions in urban areas. During winter, solar radiation is significantly reduced, especially in the higher latitudes of Southern Xinjiang. The lower sun angle results in less intense heating of urban surfaces, particularly when compared to the vast surrounding desert areas like the Taklimakan Desert. The Taklimakan Desert's sandy soil has a high heat absorption capacity during the day, leading to a more pronounced warming effect in rural areas. In contrast, urban areas with buildings, roads, and other infrastructure may absorb less solar radiation due to shading effects and the low angle of the winter sun, contributing to relatively cooler urban temperatures during the day.

In terms of UHI intensity, the study shows that temperature and precipitation are significant factors, particularly in spring and summer. The positive correlation between precipitation and daytime UHI intensity mirrors findings from previous research, such as Zhao et al. [52] on UHI effects in North America. The link between precipitation and UHI intensity can be explained by its role in altering surface moisture content, which in turn affects heat exchange processes. In Southern Xinjiang, where arid conditions prevail, even modest precipitation can exacerbate the UHI effect by creating conditions that increase heat retention in urban areas.

Unlike many other Chinese cities where nighttime UHI intensity exceeds daytime levels, Southern Xinjiang's UHI intensity is generally higher during the day, particularly in the summer. This anomaly can be attributed to the region's unique geographical and environmental conditions. The high surface albedo of the Taklimakan Desert plays a

crucial role in this dynamic. The desert's reflective surface reduces heat absorption in rural areas, while urban areas, with their lower albedo (due to roads and buildings), absorb significantly more solar radiation during the day. This differential in radiation absorption leads to heightened daytime UHI intensity. Moreover, the region's abundant solar radiation amplifies this effect, further intensifying daytime UHI during summer months.

Aerosol optical depth (AOD) also emerges as a significant factor, particularly in influencing nighttime UHI intensity. The study found that higher AOD concentrations at night were associated with stronger UHI effects. This is largely due to the scattering and absorbing properties of aerosol particles, which hinder the effective release of long-wave radiation from the urban surface at night. Instead, the radiation is scattered back toward the surface, increasing downward long-wave radiation and preventing urban temperatures from dropping significantly. The size and composition of aerosol particles further influence this process. Southern Xinjiang's urban agglomerations, characterized by frequent sandstorms and dust storms, experience high concentrations of coarse aerosol particles, which are particularly effective at scattering long-wave radiation. This phenomenon contributes to the persistence of UHI intensity during the night.

The results also highlight the need for targeted environmental management strategies to mitigate UHI effects in the region. The frequent occurrence of sand and dust storms, coupled with the region's high aerosol concentrations, suggests that efforts to control wind and sand movement could significantly reduce nighttime UHI intensity. Implementing vegetation cover and green infrastructure in and around urban areas could also help by enhancing evapotranspiration and providing shade, which would reduce the amount of heat absorbed during the day. In the long term, these measures could contribute to more sustainable urban development and improved living conditions in Southern Xinjiang.

5. Conclusions

In this paper, the spatial and temporal distribution characteristics of the heat island effect and its influencing factors in the urban agglomeration of Southern Xinjiang are studied using the data of surface temperature, air temperature, precipitation, and AOD from 2000 to 2015, and the results are as follows:

(1) The impervious surfaces in the Southern Xinjiang urban agglomeration experienced a notable increase between 1995 and 2015, and increased most rapidly between 2010 and 2015, and the growth of impervious surface in each city showed a concentrated distribution. The expansion of impervious surfaces changes the thermal characteristics of the urban environment, leading to an increase in the intensity of the urban heat island effect.

(2) There are notable spatial variations in daytime heat island intensity across the cities within the Southern Xinjiang urban sgglomeration. The highest annual average daytime heat island intensity was observed in Hotan City, reaching 3.7 °C, while the lowest was recorded in Aksu, at approximately 1.6 °C. The spatial distribution of surface temperatures in each city shows an increasing trend in the center of the city.

(3) Daytime heat island intensity of cities in the South Xinjiang urban agglomeration is characterized by obvious seasonal changes, and the seasonal trends of daytime heat island intensity are not the same in each city, though all of them show the highest heat island intensity in the summer. In 2000–2015, daytime heat island intensity in the South Xinjiang urban agglomeration showed a general upward trend, among which the upward trend in Kashgar City was the most significant. The highest nocturnal heat island intensity in each city occurs in the summer or autumn, and there are obvious differences in the trends of nocturnal heat island intensity in each city. The trends of nocturnal heat island intensity in each city in the South Xinjiang urban agglomeration are not the same in 2000–2015, and the intensity of nocturnal heat island is enhanced in most of the cities.

(4) The annual average daytime heat island intensity in the Southern Xinjiang urban agglomeration shows significant associations with nighttime light, population, im-

pervious surfaces, temperature, precipitation, and aerosol optical depth (AOD), all of which are positively correlated with UHI intensity. In contrast, the correlation between PM10 concentrations and heat island intensity is generally weak and varies across different cities and seasons.

In conclusion, this study highlights the complex interplay of geographical, meteorological, and environmental factors associated with UHI intensity in Southern Xinjiang. Temperature, precipitation, and AOD emerge as key factors, but the region's unique environmental context—dominated by the Taklimakan Desert—introduces distinctive thermal dynamics that set it apart from other urban areas. The findings of this study not only enhance our understanding of UHI patterns in arid environments but also offer valuable insights for urban planning and environmental policy formulation aimed at mitigating UHI effects in Southern Xinjiang. Considering the characteristics of the urban heat island in the South Xinjiang region and its unique natural climate environment, the following points will effectively mitigate its heat island effect: (a) Increasing green infrastructure by promoting urban greenery with drought-resistant plants, green roofs, and parks to reduce surface temperatures in the arid climate. (b) Optimizing urban design by creating wind corridors to enhance natural ventilation and mitigate heat accumulation in densely built areas. (c) Promote energy-efficient building; to minimize heat absorption and promote natural ventilation. (d) Establish continuous UHI monitoring systems and develop public education campaigns.

Author Contributions: Conceptualization, C.W. and A.M.; methodology, C.W. and H.S.; data curation, H.S., Y.W. (Yu Wang) and J.P.; writing—original draft preparation, C.W., Y.W. (Yisilamu Wulayin) and J.L.; writing—review and editing, M.S., A.A. and J.G.; visualization, C.W. and F.Y.; supervision, W.H. and C.Z.; funding, A.M. All authors have read and agreed to the published version of the manuscript.

Funding: This research was funded by the Scientific and Technological Innovation Team (Tian Shan Innovation Team) project: 2022TSYCTD0007; the Youth Innovation Team of China Meteorological Administration: CMA2024QN13; National Natural Science Foundation of China: 42375084, 42305132; China Desert Meteorology Research Foundation: Sqj2021005; Technical Service for Risk Survey of Sandstorm Meteorological Disasters in the Autonomous Region: 2023-51; Third Xinjiang Scientific Expedition: 2022xjkk030502; Funding for the Training of Key Minority Science and Technology Personnel in 2022: 2021TP130XJ; the 2024 Detection Center Observation Test Program Project: GCSYJH24-01, GCSYJH24-11; Xinjiang Uygur Autonomous Region Key Research and Development Program: 2023B02004-2; the Special Funds for Basic Scientific Research Business Expenses of Central level Public Welfare Scientific Research Institutes, grant number: IDM2021005.

Data Availability Statement: Data used in this study can be provided by Congwen (wencong@idm.cn) upon request.

Conflicts of Interest: The authors declare no conflicts of interest.

References

1. Oke, T.R. The energetic basis of the urban heat island. *Q. J. R. Meteorol. Soc.* **1982**, *108*, 1–24. [CrossRef]
2. Howard, L. *The Climate of London, Deduced from Meteorological Observations, Made at Different Places in the Neighbourhood of the Metropolis*; Cambridge University Press: Cambridge, UK, 2010; Volume I.
3. Buyantuyev, A.; Wu, J. Urban heat islands and landscape heterogeneity: Linking spatiotemporal variations in surface temperatures to land-cover and socioeconomic patterns. *Landsc. Ecol.* **2010**, *25*, 17–33. [CrossRef]
4. Bornstein, R.D. Observations of the Urban Heat Island Effect in New York City. *J. Appl. Meteorol. Climatol.* **1968**, *7*, 575–582. [CrossRef]
5. Heaviside, C.; Vardoulakis, S.; Cai, X.M. Attribution of mortality to the urban heat island during heatwaves in the West Midlands, UK. *Environ. Health* **2016**, *15*, 49–59. [CrossRef]
6. Ren, Z.; Zhao, H.; Fu, Y.; Xiao, L.; Dong, Y. Effects of urban street trees on human thermal comfort and physiological indices: A case study in Changchun city, China. *J. For. Res.* **2022**, *33*, 911–922. [CrossRef]
7. Zhou, D.C.; Xiao, J.F.; Bonafoni, S.; Berger, C.; Deilami, K.; Zhou, Y.Y.; Frolking, S.; Yao, R.; Qiao, Z.; Sobrino, J.A. Satellite Remote Sensing of Surface Urban Heat Islands: Progress, Challenges, and Perspectives. *Remote Sens.* **2019**, *11*, 48. [CrossRef]
8. Li, Y.; Zhou, D.; Yan, Z. Spatiotemporal Variations in Atmospheric Urban Heat Island Effects and Their Driving Factors in 84 Major Chinese Cities. *Environ. Sci.* **2021**, *42*, 5037–5045. (In Chinese) [CrossRef]

9. Xu, Y.; Liu, Y. Monitoring the Near-surface Urban Heat Island in Beijing, China by Satellite Remote Sensing. *Geogr. Res. J. Inst. Aust. Geogr.* **2015**, *53*, 16–25. [CrossRef]
10. Chen, Y.; Sun, H.; Li, J. Estimating daily maximum air temperature with MODIS data and a daytime temperature variation model in Beijing urban area. *Remote Sens. Lett.* **2016**, *7*, 865–874. [CrossRef]
11. Peng, J.; Xie, P.; Liu, Y.; Ma, J. Urban thermal environment dynamics and associated landscape pattern factors: A case study in the Beijing metropolitan region. *Remote Sens. Environ.* **2016**, *173*, 145–155. [CrossRef]
12. Feng, J.; Cai, X.; Chapman, L. Impact of atmospheric conditions and levels of urbanisation on the relationship between nocturnal surface and urban canopy heat islands. *Q. J. R. Meteorol. Soc.* **2019**, *145*, 3284–3299. [CrossRef]
13. Wen, C.; Mamtimin, A.; Feng, J.; Wang, Y.; Yang, F.; Huo, W.; Zhou, C.; Li, R.; Song, M.; Gao, J.; et al. Diurnal Variation in Urban Heat Island Intensity in Birmingham: The Relationship between Nocturnal Surface and Canopy Heat Islands. *Land* **2023**, *12*, 2062. [CrossRef]
14. Tian, P.; Li, J.; Cao, L.; Pu, R.; Wang, Z.; Zhang, H.; Chen, H.; Gong, H. Assessing spatial characteristics of urban heat islands from the perspective of an urban expansion and ecological landscape. *Sustain. Cities Soc.* **2021**, *74*, 103208. [CrossRef]
15. Hu, L.; Nathaniel, A.B. The impact of temporal aggregation of land surface temperature data for surface urban heat island (SUHI) monitoring. *Remote Sens. Environ.* **2013**, *134*, 162–174. [CrossRef]
16. Cao, C.; Li, X.; Zhang, M. Correlation Analysis of the Urban Heat Island Effect and Its Impact Factors in China. *Environ. Sci.* **2017**, *38*, 3987–3997. (In Chinese)
17. Hu, N.; Ren, Z.; Dong, Y.; Fu, Y.; Guo, Y.; Mao, Z.; Chang, X. Spatiotemporal evolution of heat island effect and its driving factors in urban agglomerations of China. *Sci. Geogr. Sin.* **2022**, *42*, 1534–1545. (In Chinese) [CrossRef]
18. Jaiswal, T.; Jhariya, D.; Singh, S. Spatio-temporal analysis of changes occurring in land use and its impact on land surface temperature. *Environ. Sci. Pollut. Res.* **2023**, *30*, 107199–107218. [CrossRef]
19. Cecilia, A.; Casasanta, G.; Petenko, I.; Conidi, A.; Argentini, S. Measuring the urban heat island of Rome through a dense weather station network and remote sensing imperviousness data. *Urban Clim.* **2023**, *47*, 101355. [CrossRef]
20. Zargari, M.; Mofidi, A.; Entezari, A.; Baaghideh, M. Climatic comparison of surface urban heat island using satellite remote sensing in Tehran and suburbs. *Sci. Rep.* **2024**, *14*, 643. [CrossRef]
21. Xi, Y.; Wang, S.; Zou, Y.; Zhou, X.; Zhang, Y. Seasonal surface urban heat island analysis based on local climate zones. *Ecol. Indic.* **2024**, *159*, 111669. [CrossRef]
22. Min, M.; Zhao, H.; Miao, C. Spatio-Temporal Evolution Analysis of the Urban Heat Island: A Case Study of Zhengzhou City, China. *Sustainability* **2018**, *10*, 1992. [CrossRef]
23. Yang, Q.; Xu, Y.; Wen, D.; Hu, T.; Chakraborty, T.C.; Liu, Y.; Yao, R.; Chen, S.; Xiao, C.; Yang, J. Satellite Clear-Sky Observations Overestimate Surface Urban Heat Islands in Humid Cities. *Geophys. Res. Lett.* **2024**, *51*, e2023GL106995. [CrossRef]
24. Feng, H.; Zhao, X.; Chen, F.; Wu, L. Using land use change trajectories to quantify the effects of urbanization on urban heat island. *Adv. Space Res.* **2014**, *53*, 463–473. [CrossRef]
25. Silva, R.; Carvalho, A.C.; Carvalho, D.; Rocha, A. Study of Urban Heat Islands Using Different Urban Canopy Models and Identification Methods. *Atmosphere* **2021**, *12*, 521. [CrossRef]
26. Almeida, C.R.d.; Teodoro, A.C.; Gonçalves, A. Study of the Urban Heat Island (UHI) Using Remote Sensing Data/Techniques: A Systematic Review. *Environments* **2021**, *8*, 105. [CrossRef]
27. Hidalgo-García, D.; Arco-Díaz, J. Modeling the Surface Urban Heat Island (SUHI) to study of its relationship with variations in the thermal field and with the indices of land use in the metropolitan area of Granada (Spain). *Sustain. Cities Soc.* **2022**, *87*, 104166. [CrossRef]
28. Assaf, G.; Assaad, R.H. Modeling the impact of land use/land cover (LULC) factors on diurnal and nocturnal Urban Heat Island (UHI) intensities using spatial regression models. *Urban Clim.* **2024**, *55*, 101971. [CrossRef]
29. Tehrani, A.A.; Veisi, O.; Kia, K.; Delavar, Y.; Bahrami, S.; Sobhaninia, S.; Mehan, A. Predicting urban Heat Island in European cities: A comparative study of GRU, DNN, and ANN models using urban morphological variables. *Urban Clim.* **2024**, *56*, 102061. [CrossRef]
30. Anniballe, R.; Bonafoni, S.; Pichierri, M. Spatial and temporal trends of the surface and air heat island over Milan using MODIS data. *Remote Sens. Environ.* **2014**, *150*, 163–171. [CrossRef]
31. Chapman, S.; Thatcher, M.; Salazar, A.; Watson, J.E.; McAlpine, C.A. The impact of climate change and urban growth on urban climate and heat stress in a subtropical city. *Int. J. Climatol.* **2019**, *39*, 3013–3030. [CrossRef]
32. Cao, C.; Lee, X.; Liu, S.; Schultz, N.; Xiao, W.; Zhang, M.; Zhao, L. Urban heat islands in China enhanced by haze pollution. *Nat. Commun.* **2016**, *7*, 12509. [CrossRef] [PubMed]
33. Zhao, L.; Lee, X.; Smith, R.B.; Oleson, K. Strong contributions of local background climate to urban heat islands. *Nature* **2014**, *511*, 216–219. [CrossRef] [PubMed]
34. Lai, J.; Zhan, W.; Voogt, J.; Quan, J.; Huang, F.; Zhou, J.; Bechtel, B.; Hu, L.; Wang, K.; Cao, C.; et al. Meteorological controls on daily variations of nighttime surface urban heat islands. *Remote Sens. Environ.* **2020**, *253*, 112198. [CrossRef]
35. Fan, J.; Chen, X.; Sun, J. Research progress on heat island effect of oasis cities in arid zone of northwest China. *Environ. Prot. Sci.* **2024**, *50*, 9–14. [CrossRef]
36. Wang, S.; Alishir, K.; Guo, Y.; Duan, H.M. Study on Temperature Change and Urban Heat Island Effect in the Urumqi Region. *Arid Zone Res.* **2009**, *26*, 433–440. [CrossRef]

37. Gulbakram, A.; Zan, M. The Influence of Heat Island Effect on Vegetation Phenology in Major Urban Clusters in the Tianshan Northslope Economic Belt of Xingjiang. *J. Ecol. Rural Environ.* **2022**, *38*, 872–881.
38. Walijiang, W.; Ren, G.; Sun, X. The Daily Temperature Characteristics of the Intensity of Urban Heat Island in Urumqi and Seasonal Changes. *Desert Oasis Meteorol.* **2018**, *12*, 21–28. (In Chinese)
39. Abulimiti, A.; Liu, Y.; Tang, J.; Mamtimin, A.; Yao, J.; Zeng, Y.; Abulikemu, A. Urbanization Effect on Regional Thermal Environment and Its Mechanisms in Arid Zone Cities: A Case Study of Urumqi. *Remote Sens.* **2024**, *16*, 2939. [CrossRef]
40. Hussein, N.M.; Assaf, M.N. Assessment of spatial and temporal distribution of Urban Heat Islands (UHI) in semi-arid climate. *J. Environ. Eng. Landsc. Manag.* **2023**, *31*, 52–66. [CrossRef]
41. Gourfi, A.; Taïbi, A.N.; Salhi, S.; Hannani, M.E.; Boujrouf, S. The Surface Urban Heat Island and Key Mitigation Factors in Arid Climate Cities, Case of Marrakesh, Morocco. *Remote Sens.* **2022**, *14*, 3935. [CrossRef]
42. Espinoza-Molina, J.; Acosta-Caipa, K.; Chambe-Vega, E.; Huayna, G.; Pino-Vargas, E.; Abad, J. Spatiotemporal Analysis of Urban Heat Islands in Relation to Urban Development, in the Vicinity of the Atacama Desert. *Climate* **2022**, *10*, 87. [CrossRef]
43. Rajeswari, J.R.; Fountoukis, C.; Siddique, A.; Moosakutty, S.; Mohieldeen, Y.; Ayoub, M.A.; Alfarra, M.R. Urban heat island phenomenon in a desert, coastal city: The impact of urbanization. *Urban Clim.* **2024**, *56*, 102016. [CrossRef]
44. Gulnur, A.; Ali, M.; Wang, Y. Analysis on Literature of Sandstorm in the Taklimakan Desert Based on VOSviewer. *Desert Oasis Meteorol.* **2023**, *17*, 8–14. (In Chinese)
45. Ali, M.; Huo, W.; Yang, X.; Wang, M. Research Advance of Sandstorm in Xinjiang. *Desert Oasis Meteorol.* **2022**, *16*, 1–7. (In Chinese)
46. Yang, J.; Huang, X. The 30 m annual land cover dataset and its dynamics in China from 1990 to 2019. *Earth Syst. Sci. Data* **2021**, *13*, 3907–3925. [CrossRef]
47. Wei, J.; Li, Z. *ChinaHighPM2.5: High-Resolution and High-Quality Ground-Level PM2.5 Dataset for China (2000–2023)*; National Tibetan Plateau/Third Pole Environment Data Center: Beijing, China, 2023. [CrossRef]
48. Wei, J.; Li, Z.; Xue, W.; Sun, L.; Fan, T.; Liu, L.; Su, T.; Cribb, M. The ChinaHighPM10 dataset: Generation, validation, and spatiotemporal variations from 2015 to 2019 across China. *Environ. Int.* **2021**, *146*, 106290. [CrossRef]
49. Peng, S. *1-Km Monthly Precipitation Dataset for China (1901–2023)*; National Tibetan Plateau/Third Pole Environment Data Center: Beijing, China, 2020. [CrossRef]
50. Gong, P.; Li, X.; Wang, J.; Bai, Y.; Chen, B.; Hu, T.; Liu, X.; Xu, B.; Yang, J.; Zhang, W.; et al. Annual maps of global artificial impervious area (GAIA) between 1985 and 2018. *Remote Sens. Environ.* **2020**, *236*, 111510. [CrossRef]
51. Platnick, S.; King, M.; Hubanks, P. *MODIS Atmosphere L3 Daily Product, NASA MODIS Adaptive Processing System, Goddard Space Flight Center, USA*; NASA: Washington, DC, USA, 2015. [CrossRef]
52. Zhou, D.; Zhao, S.; Liu, S.; Zhang, L.; Zhu, C. Surface urban heat island in China's 32 major cities: Spatial patterns and driver. *Remote Sens. Environ.* **2014**, *152*, 51–61. [CrossRef]

Disclaimer/Publisher's Note: The statements, opinions and data contained in all publications are solely those of the individual author(s) and contributor(s) and not of MDPI and/or the editor(s). MDPI and/or the editor(s) disclaim responsibility for any injury to people or property resulting from any ideas, methods, instructions or products referred to in the content.